

# Visualization of Cervical Cancer Classification using Deep Convolutional Neural Network

C.Dharani, S.Kaviya, S.Maheshwari, K.Monisha,

*Department of ECE,*

*Kongunadu College of Engineering and Technology, Thottiyam, Tamilnadu, India*

P.Elayaraja

*Associate Professor,*

*Kongunadu College of Engineering and Technology, Thottiyam, Tamilnadu, India*

**Abstract - Cervical cancer is the fourth most prevalent disease in women. Accurate and timely cancer detection can save lives. Automatic and reliable cervical cancer detection methods can be devised through the accurate segmentation and classification of Pap smear cell images. This paper presents an approach to whole cervical cell segmentation and classification using a Deep Convolutional Neural Network. We evaluate our proposed method on the Guanacaste dataset containing Pap smear images. In the segmentation phase, when Mask R-CNN is applied on the whole cell, it outperforms the previous segmentation method in precision ( $0.92\pm 0.06$ ), recall ( $0.91\pm 0.05$ ) and ZSI ( $0.91\pm 0.04$ ). In the classification phase, DCNN approach is applied on the whole segmented cell. The DCNN method gives information about the cancer type and their severity.**

**Keywords - Mask R-CNN, DCNN, Cell Segmentation, Cell Classification, Pap Smear Images**

## I. INTRODUCTION

Cancer is a life-threatening disease and has become a major burden worldwide. Global cancer data reveals that cervical cancer is the fourth most prevalent disease among females, with an approximately 90% fatality rate in underdeveloped and developing nations due to the absence of public knowledge of its causes and impacts. Fortunately, this lethal disease can be detected by the regular Pap smear testing of the cervical cells. The cell samples which are collected at the outer opening of the cervix are placed on a glass tube and stained by a pathologist for examination under a microscope to determine if there are any defects/abnormalities that indicate a pre-cancerous phase.

Manual cell screening often results in large variations in the quality of specimens, such as the uneven distribution of the cellular material that can lead to dense clumps which light cannot penetrate whereas other parts of the specimen may have many overlapping cells which hinders an accurate interpretation. Moreover, a manual visual examination is time consuming and the analysis and classification of hundreds or thousands of cells can be inaccurate due to human error. When cell examination for abnormality is carried out by a computer, the cell must be scanned at high resolution to reliably extract the features. Due to size and shape variations of normal and abnormal cells, accurate cell segmentation and classification is crucial to differentiate between normal and abnormal cells.

The aim of this paper is to develop a better system for the automatic detection of cancer cells using a deep learning approach on Pap smear images. Deep learning techniques can be used to identify patterns in complex big data starting with preprocessing the data, training the model and testing it. The primary contributions of this paper are as follows. As far as we know, this work is the first to implement Mask R-CNN and the transfer learning technique to segment the whole cervical cell. As far as we are aware, this work is the first to implement a DCNN approach in which the whole cervical cells are classified.

## II. METHODOLOGY

The cervical images used in this paper are obtained from Guanacaste dataset (2005). This dataset contains large numbers of cervical Pap Smear images with its corresponding ground truth images, which are marked by expert radiologist. In this paper, the images from this dataset are automatically classified into various severity classifications steps. The first stage partitions the cell regions using Mask R-CNN segmentation. The second

stage defines the whole cell area (nucleus and cytoplasm) by classifying the segments from the initial stage. The classification in the second phase includes training and testing phase as shown in Figure 1.

#### A.DATASET:

TABLE 1: Distribution of 7-classes of Pap Smear Images.

CLASS	CELL TYPE	CELL COUNT	CATEGORY
1	SUPERFICIAL SQUAMOUS EPITHELIAL	74	NORMAL
2	INTERMEDIATE SQUAMOUS EPITHELIAL	70	NORMAL
3	COLUMNAR EPITHELIAL	98	NORMAL
4	MILD SQUAMOUS NON KERATINIZING DYSPLASIA	182	ABNORMAL
5	<i>MODERATE</i> SQUAMOUS NON KERATINIZING DYSPLASIA	146	ABNORMAL
6	<i>SEVERE</i> SQUAMOUS NON KERATINIZING DYSPLASIA	197	ABNORMAL
7	SQUAMOUS CELL <i>CARCINOMA IN SITU INTERMEDIATE</i>	150	ABNORMAL

**B.PROPOSED METHOD:**

The objective of this work is to develop a method to segment whole cervical cells, both single and overlapping, from conventional Pap smear images, and then classify them to identify normal and abnormal cells. The proposed method comprises two

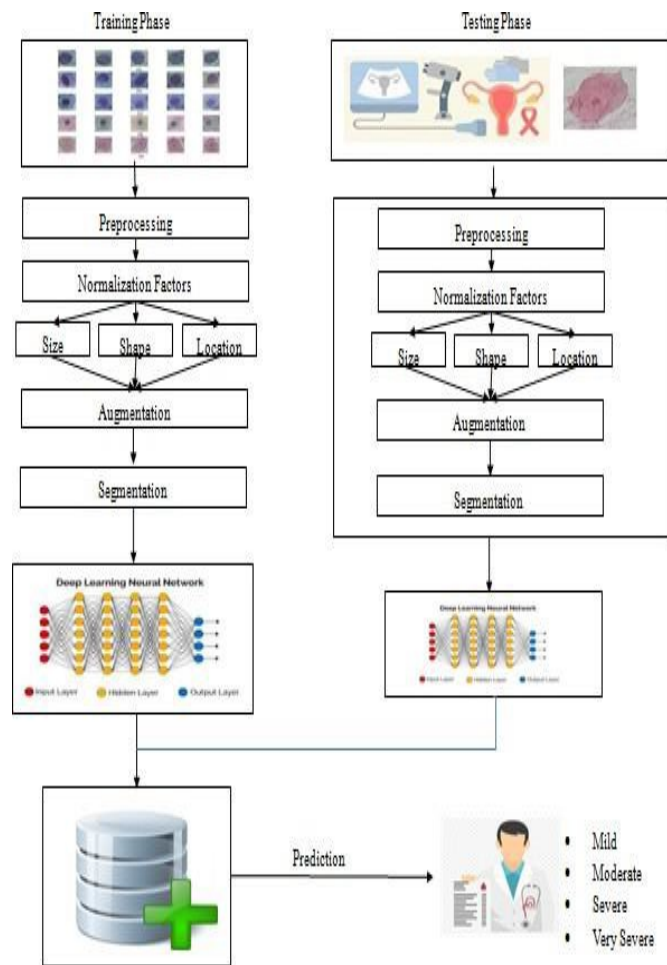


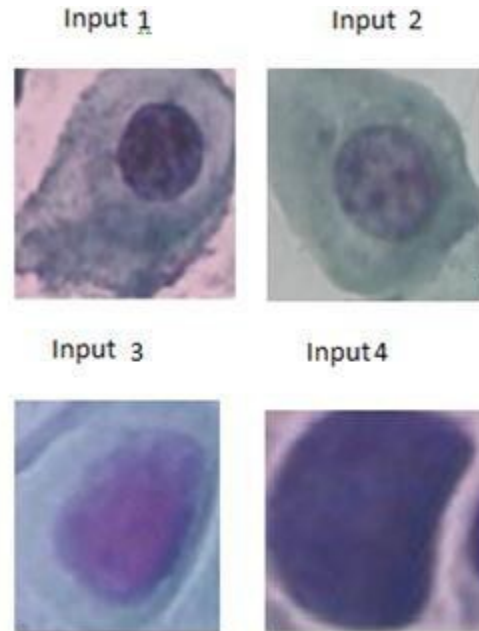
Fig 1: Proposed system Architecture

**B.1 PRE PROCESSING:**

The training phase in segmentation and classification has a different preprocessing scheme. In the segmentation stage, preprocessing begins by separating the image data of the cervical cell from its mask. In the case of the dataset that we use, the original image and mask data are still mixed in one folder which corresponds to the cancer class name. This collection of images is read based on the file name pattern and is then separated into

only two types of images, namely the original image of the cervical cell and the mask. When the preprocessing application finds that what is being read is a mask image, the image will be converted into a binary image, that is, white for pixels which are a part of the cervical cells (a combination of cell nuclei and cytoplasm) and black for the other pixels. The original image of the cervical cell and its binary mask image is then resized into 200 pixels with a length that is proportionally adjusted based on the new width. The two groups of images are ready for further processing, namely network training using Mask R-CNN.

Fig 2 : Input images for Preprocessing.



## B.2.NORMALIZATION FACTOR:

### B.2.1.SIZE:

a) Area of nucleus and cytoplasm: The number of pixels in the nucleus and cytoplasm respectively are counted to determine their area.

b) N/C ratio: The size of the nucleus with respect to cytoplasm determines the severity of cancer. The benign cells have small, round and compact nucleus located in the center of the cytoplasm. The cancer cells have a larger, irregularly shaped and sparse nucleus whose center deviates from the center of nucleus. The N/C ratio is a foremost feature deciding the nature of cells.

$$N/C = \text{Nuclarea}/(\text{Nuclarea}+\text{Cytoarea})$$

c) Minor and Major axes length: These measurements of the vital components of image decide the roundness of the nucleus and cytoplasm. The minor axis forms the smallest diameter and major axis forms the largest diameter.

### B.2.2.SHAPE:

a) Perimeter of cytoplasm and nucleus: The number of pixels that lie along the border are added up to form the perimeter.

### B.2.3.LOCATION :

The distance between the centroids of nucleus and cytoplasm is also used to determine the malignancy of cells.

### B.3.AUGMENTATION :

The aim of applying data augmentation is to increase the generalizability of the model which can increase the dataset size and classification accuracy while preventing overfitting. In this study, data augmentation is used both in the segmentation training phase and the classification training phase. We used several geometric transformation methods on the Guanacaste dataset for data augmentation, i.e. top- down translation, left-right translation, horizontal reflection, vertical reflection and rotation. For each training data image, the application will select randomly what kind of geometric transformations will be applied to the image. Figure 2 shows the augmented data results for classification using 30-degree rotations and 5 pixels of translation applied on the Guanacaste dataset.

### B.4.SEGMENTATION:

There are three primary goals of object detection i.e., given an input image to obtain

- 1) A list of bounding boxes for each object in the image,
- 2) A class label associated with each bounding box and
- 3) The confidence score associated with each bounding box and class label.

Instance segmentation takes object detection a step further. Instead of predicting a bounding box for each object in an image, we now want to predict a mask for each object, giving us a pixel-wise segmentation of the object rather than a coarse, perhaps even unreliable bounding box. Instance segmentation algorithms attempt to partition the image into meaningful parts and associate every pixel in an boxes around each instance of a class and then performing semantic segmentation on each of input image with a class label (e.g., person, road, car, bus). While object detection produces a bounding box, instance segmentation produces a pixel-wise mask for each individual object. However, instance segmentation does not require every pixel in an image to be associated with a label. Instance segmentation can be solved using two steps, i.e., performing object detection to draw bounding the bounding boxes.

Fig 3: Segmented images

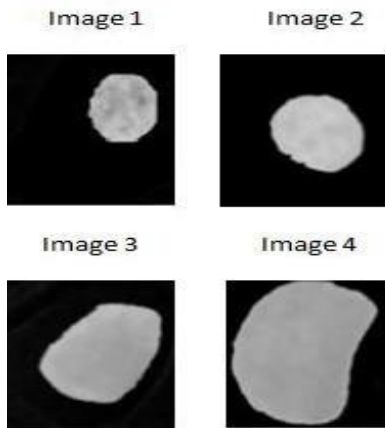
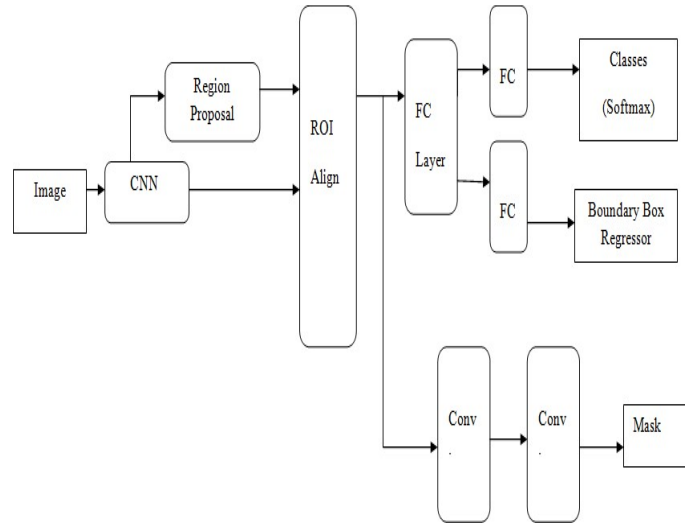


Fig 4: Mask R-CNN Architecture



### B.5.CLASSIFICATION:

In this section, we explore different strategies and scenarios for the classification of nuclei in cervical cell images.

#### B.5.1. Multi-class classification using transfer learning:

Considering the success of deep learning methodologies in recent years for the task of classification, we too explore their application in our work. The PAP-smear images generally have a large appearance variation in terms of both contrast and color in the normal and abnormal cells. Furthermore, in medical imaging applications, very few annotated images are available, in the range of hundreds, as opposed to the millions of natural images available for other applications. To overcome the aforementioned difficulties, we make use of the concept of transfer learning where the filters learned by a CNN, retrained on Image Net consisting of millions of images, are directly used for classification in some other domain (medical images in our case). This strategy helps us in two ways:

- 1) It mitigates the dependency of deep CNNs on huge amount of annotated training data.
- 2) It effectively reduces the training time required for training a CNN from scratch.

It is shown in literature that the lower level convolutional layers learn the low-level primitive features such as gradients, texture etc., and the deeper layers, learn the high-level data septic semantic features. Considering the hypothesist that semantic features may not be important for cell classification, we explore for classification, the outputs from the filters learned by Alexnet at last (conv5), intermediate (conv3) and first (conv1) convolutional layers followed by two fully connected layers which we retrain, one consisting of 256 neurons and the last layer consisting of number of neurons equal to number of classes. We refer to these new transfer-learning based networks in the rest of the paper as conv5T (Figure 5)

Fig 5 : Conv5:Fivth convolutional layer features

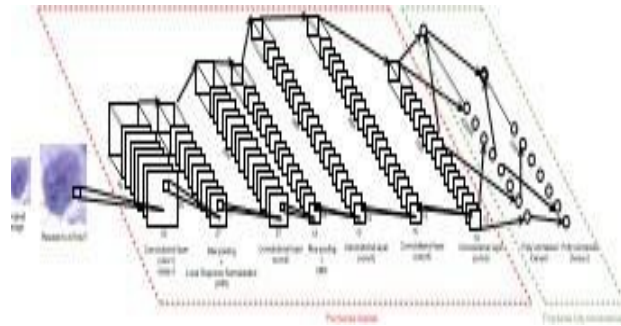


Fig 6: Conv3:Third convolutional layer features

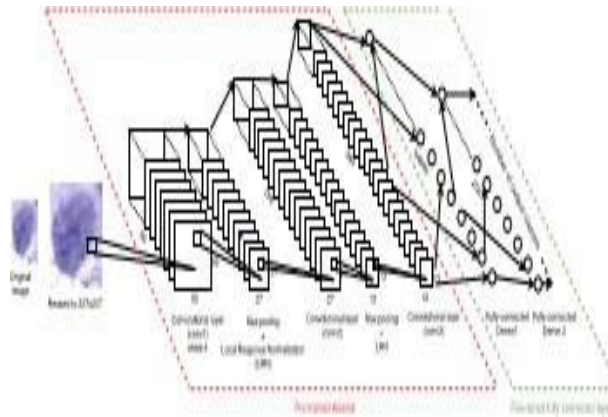
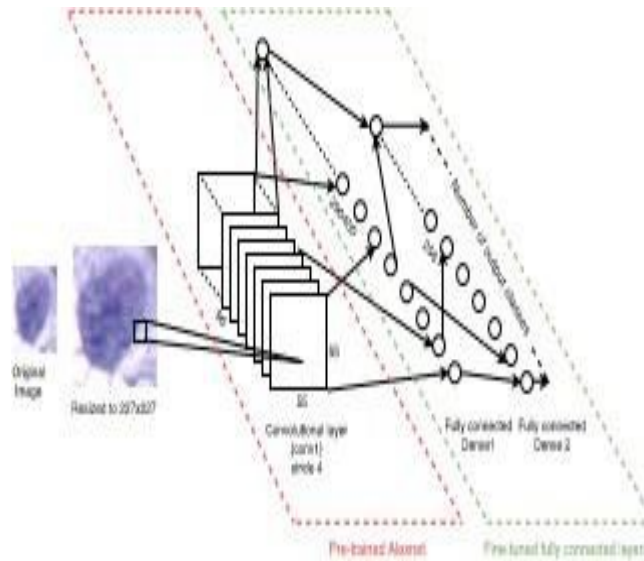


Fig 7:Conv1: First Convolutional layer features

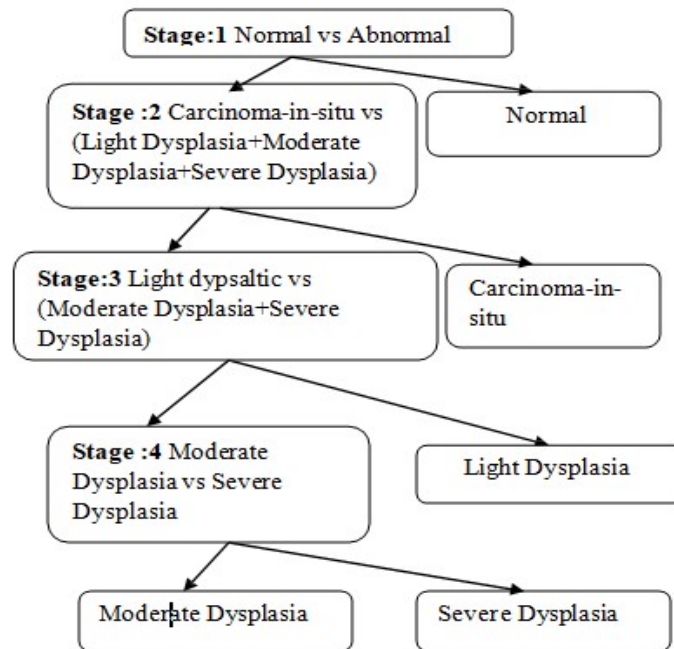


B.5.2. Decision-tree based classification using transfer learning:

Considering certain similarities and differences between some classes, we propose a decision-tree based approach

for classifying the cell images in a hierarchical way as shown in Figure 7. At the first node, a two-class classification is done between the normal and abnormal classes. This is also important from the perspective of a screening system where only the difference between normal and abnormal classes can also be considered important. Additionally, once we have a good classification between the normal and abnormal class, we can classify the abnormal cells into further gradations of abnormalities. We achieve this in the daughter nodes where at the second level we discriminate between the highest level of abnormal class with other classes. Next, we discriminate between the lowest level of abnormal class with the remaining classes. Finally, at the leaf node, we discriminate between the leftover abnormal classes. The number of levels in the tree is based on the number of gradations of abnormalities in the dataset of the cervical images.

Fig 8: Decision Tree Based Approach for Classification



#### B.5.3. Classification of detected nuclei in multi-cell images using transfer learning:

Following the success of CNN-based classification approach, we apply the transfer learning based methodology to the real-world multi-cell PAP-smear images. After detecting the nuclei with the help of detection algorithm mentioned, we extract the detected nuclei regions as sub images using bounding boxes around the connected components. These sub-images are now passed on for classification to a CNN whose features for the first convolutional layer are extracted directly from the first convolutional layer of the pre-trained Alexnet. Because there can be large variations in multi-cell images, over fitting can occur. To reduce the chances of over fitting, we use two techniques:

- 1) By appending a few untrained convolutional layers before the fully connected layers, the number of nodes in the fully connected layers is reduced and hence the number of parameters to be trained in the network are reduced.
- 2) Using max-pooling dropout after every untrained convolutional layer

#### B.5.4. Classification with segmented nuclei:

For classification on segmented nuclei images with conv1T architecture. From the detected cells, the nuclei is segmented and the background values are replaced by 255. These images are now fed into the conv1T architecture, assisting it by emphasizing the nucleus features. Here, we also pose the question if the exact segmentation is needed for classification and demonstrate the answer through experimentation with and without segmentation of nuclei in single-cell image.

### III. RESULT A.Cervical Cell Segmentation:

The objective of cervical segmentation is to divide a cell into two areas, i.e., the whole cell which consists of the cytoplasm and nucleus, and the background. Sample images from the Guanacaste data set at every phase in the Mask-RCNN Segmentation are shown in Figure6. The original images were masked with a white color for cytoplasm and nuclei, and black for the background.

As seen in Figure 8, the image source column is the cervical cell images taken from the dataset as is, without any image processing. The original mask is converted from the ground truth mask (from color to a binary image) provided in the original Guanacaste dataset. This converted mask will be used to train the Mask R-CNN and to measure the quality of our network. The predicted mask is the binary mask generated by the trained Mask-RCNN while the overlaid image shows the area from the image source which is predicted as the cell area and will be fed to the DCNN network.

Our proposed segmentation using Mask R-CNN produces high average performance, i.e. 92% precision,91% recall and 91% ZSI for all cell types with low standard deviation. Only the normal columnar type produces a performance result below 90%.

### B:Cervical Cell Classification:

#### B.1.With detected nuclei using transfer learning:

For multiclass classification using transfer learning, we explore the architectures conv5T, conv3T and conv1T given in Figure 4, 5 and 6 where we use the outputs from the fifth, third and first convolutional layers of Alexnet, respectively. After getting the respective outputs from pre-trained Alexnet, we train the fully connected layers with a 256-neuron hidden layer and a final output layer with number of neurons equal to the number of classes. Because of high dimensional outputs from the convolution layers of Alexnet, the number of weights to be trained are huge (in the range of 1 million), hence we use data augmentation on the training data. We also use data augmentation on validation data to reduce the extreme fluctuations in validation accuracy while training.

After this, we end up with 12,000 examples for training and 3000 for validation. We use 5 random sets of training, validation and testing data for the experimentation and report the average results in Figure 9. All three of these networks are trained for

200 epochs and mean squared error as loss function. Activation map from different convolutional layers of Alexnet for an example image are shown in Figure

10. It can be seen that the activation map from the first convolutional layer learns the prominent texture features from the images as opposed to the third and fifth convolutional layers. This observation supports the hypothesis that for cell images, as the depth of the network increases, the high-level features do not seem informative. This also supports our motivation to select Alexnet consisting of smaller number of layers. We provide the average training, validation and testing accuracies for the 7-class classification, over 5 random trials for different architectures in Figure 9. The constant increase in accuracies from conv5T to conv1T shows that the cell classification problem performs better with low-level features rather than those at the deeper levels. We believe this is an interesting and important in sight,as typical deep learning approaches only consider the last layer features for classification.

B.2. With detected nuclei using decision-tree:

Next, we explore the results of decision-tree based classification using transfer learning. Because of the transfer learning with conv1T giving the best results, we report the decision-tree based classification results with the architecture given in Figure 6. The overall accuracies at each stage with transfer learning are given in Table VI. We note that the decision-tree based method with transfer learning gives high accuracy at each stage.

Table 2: Accuracies at different stage of Decision-tree based approach using traditional and Deep learning based methods.

	Stage 1	Stage 2	Stage 3	Stage 4
Conv 1T	99.6%	95.6%	95.1%	94.1%

Fig 9: Resulting images

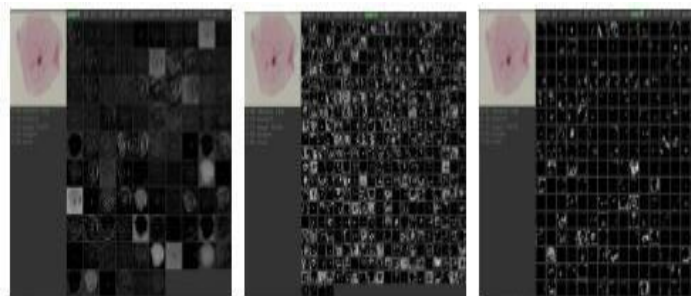
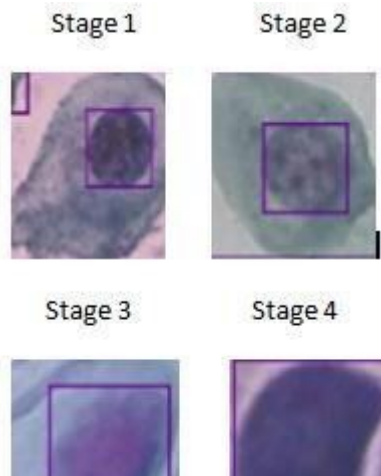


Fig 10: Activation maps: Left to Right: Conv1, Conv3 activation maps for Normal superficial cell images.

IV.CONCLUSION

In this paper, we reported a PAP-smear image analysis system for cervical cancer screening for both single and multicell images. The image analysis generally consists of three steps: detection, segmentation and classification.

We propose a simple nuclei detection algorithm for multi-cell images, and a mask R-CNN approach with selective pre-processing for segmentation. This approach results in an overall F-score of 0.90 on dataset. For classification, we propose feature level analysis using DCNN on both single and multi-cell images. A decision-tree based classification is proposed as an alternative to the multi-class classification. Further, we prove through experimentation that accurate segmentation is not necessary for classification with deep learning. We obtain state-of-the-art classification accuracy on dataset for 2-class (99.3%) and for 7-class classification (93.75%).

## REFERENCES

- [1] F. Bray, J. Ferlay, I. Soerjomataram, R. L. Siegel, L. A. Torre, and A. Jemal, "Global cancer statistics 2018: GLOBOCAN estimates of incidence and mortality worldwide for 36 cancers in 185 countries," *CA, Cancer J. Clin.*, vol. 68, no. 6, pp. 394–424, 2018.
- [2] E. Martin, "Pap-smear classification," M.S. thesis, Dept. Automat., Tech. Univ. Denmark, Lyngby, Denmark, 2003.
- [3] D. L. Rosenthal, "Computerized scanning devices for Pap smears screening: Current status and critical review," *Clinics Lab. Med.*, vol. 17, no. 2, pp. 263–284, Jun. 1997.
- [4] E. Bengtsson and P. Malm, "Screening for cervical cancer using automated analysis of PAP-smears," *Comput. Math. Methods Med.*, vol. 2014, pp. 1–12, Mar. 2014.
- [5] M. E. Plissiti, C. Nikou, and A. Charchanti, "Automated detection of cell nuclei in Pap smear images using morphological reconstruction and clustering," *IEEE Trans. Inf. Technol. Biomed.*, vol. 15, no. 2, pp. 233–241, Mar. 2011.
- [6] Y.-F. Chen, P. C. Huang, K. C. Lin, H. H. Lin, L. E. Wang, C. C. Cheng, T. P. Chen, Y. K. Chan, and J. Y. Chiang, "Semi-automatic segmentation and classification of pap smear cells," *IEEE J. Biomed. Health Informat.*, vol. 18, no. 1, pp. 94–108, Jan. 2014.
- [7] J. Su, X. Xu, Y. He, and J. Song, "Automatic detection of cervical cancer cells by a two-level cascade classification system," *Anal. Cellular Pathol.*, vol. 2016, pp. 1–11, Apr. 2016.
- [8] B. Jan, H. Farman, M. Khan, M. Imran, I. U. Islam, A. Ahmad, S. Ali, and G. Jeon, "Deep learning in big data Analytics: A comparative study," *Comput. Electr. Eng.*, vol. 75, pp. 275–287, May 2019.
- [9] R. F. Costa, A. Longatto-Filho, C. Pinheiro, L. C. Zeferino, and J. H. Fregnani, "Historical analysis of the Brazilian cervical cancer screening program from 2006 to 2013: A time for reflection," *PLoS One*, vol. 10, no. 9, Sep. 2015, Art. no. e0138945.
- [10] C. Bergmeir, M. G. Silvente, J. E. López-Cuervo, and J. M. Benítez, "Segmentation of cervical cell images using mean-shift filtering and morphological operators," *Proc. SPIE, Med. Imag., Image Process.*, vol. 7623, Mar. 2010, Art. no. 76234C. doi: 10.1117/12.845587.
- [11] W. Wu and H. Zhou, "Data-driven diagnosis of cervical cancer with support vector machine-based approaches," *IEEE Access*, vol. 5, pp. 25189–25195, 2017.
- [12] W. Wu and H. Zhou, "Data-driven diagnosis of cervical cancer with support vector machine-based approaches," *IEEE Access*, vol. 5, pp. 25189–25195, 2017.
- [13] D. Kashyap, A. Somani, J. Shekhar, A. Bhan, M. K. Dutta, R. Burget, and K. Riha, "Cervical cancer detection and classification using independent level sets and multi SVMs," in *Proc. 39th TSP*, Jun. 2016, pp. 523–528.
- [14] J. W. Zhang, S. S. Zhang, G. H. Yang, D. C. Huang, L. Zhu, and D. F. Gao, "Adaptive segmentation of cervical smear image based on GVF Snake model," in *Proc. ICMLC*, Jul. 2013, pp. 890–895.
- [15] R. R. Kumar, V. A. Kumar, P. N. S. Kumar, S. Sudhamony, and R. Ravindrakumar, "Detection and removal of artifacts in cervical cytology images using Support Vector Machine," in *Proc. ITiME*, Dec. 2012, pp. 717–721.
- [16] Y. Wang, D. Crookes, O. S. Eldin, S. Wang, P. Hamilton, and J. Diamond, "Assisted diagnosis of cervical intraepithelial neoplasia (CIN)," *IEEE J. Sel. Topics Signal Process.*, vol. 3, no. 1, pp. 112–121, Feb. 2009.
- [17] J. Jantzen, J. Norup, G. Dounias, and B. Bjerregaard, "Pap-smear benchmark data for pattern classification," in *Proc. NiSIS*, Oct. 2005, pp. 1–9.
- [18] M. Sharma, S. Kumar Singh, P. Agrawal, and V. Madaan, "Classification of clinical dataset of cervical cancer using KNN," *Indian J. Sci. Technol.*, vol. 9, no. 28, pp. 1–5, Jul. 2016.
- [19] R. Kumar, R. Srivastava, and S. Srivastava, "Detection and classification of cancer from microscopic biopsy images using clinically significant and biologically interpretable features," *J. Med. Eng.*, vol. 2015, pp. 1–14, Apr. 2015.
- [20] J. Talukdar, C. Kr Nath, and P. H. Talukdar, "Fuzzy clustering based image segmentation of Pap smear images of cervical cancer cell using FCM Algorithm".